Mon. Not. R. Astron. Soc. **000**, 000–000 (0000) Printed 23 December 2015 (MN LATEX style file v2.2)

Estimating dark matter halo concentration using the integrated mass profile

C. N. Poveda-Ruiz ⋆[1] J. E. Forero-Romero †[1] J. C. Muñoz-Cuartas ‡[2]

[1] *Departamento de Física, Universidad de los Andes, Cra. 1 No. 18A-10, Edificio Ip, Bogotá, Colombia*
[2] *Instituto de Física - FCEN, Universidad de Antioquia, Calle 67 No. 53-108, Medellín, Colombia*

23 December 2015

ABSTRACT

We present a new algorithm to estimate the concentration of N-body dark matter halos using the integrated mass profile. The method uses the full particle information without any binning, making it realiable in cases when low numerical resolution becomes a limitation for other methods. Additionally, the algorithm is straightforward to implement. We test the performance of this method by estimating halo concentration both on mock and N-body halos. We compare these results against two other methods: maximum radial velocity measurements and radial particle binning to fit the density profile. Tests on the mock halos show that the accuracy of our method to recover known input concentrations varies with halo resolution, outperforming the other two methods. For halos sampled with 20 particles our method recovers the input concentration with 10% accuracy, while for the maximum radial velocity method it is on the order of 20% and density profile methods fail at the 100% level. For halos with 2×10^4 particles our method achieves a recovery accuracy of 0.01% while the velocity and density profile methods achieve 0.1% and 1%, respectively. We also measure the mass-concentration relationship on N-body data. We find that in the probed mass range ($10^{12}h^{-1}\mathrm{M}_\odot < 10^{14}h^{-1}\mathrm{M}_\odot$) the three methods give consistent results within the statistical uncertainties. We only find a small deviation at low masses, $M < 10^{13}h^{-1}\mathrm{M}_\odot$, where our method yields lower median concentration values by $15\%-20\%$ compared to the velocity and density methods. From these results we believe that the new method is a promising tool to probe the internal structure of dark matter halos.

Key words: Cosmology: theory - large-scale structure of Universe - Methods: data analysis - numerical - N-body simulations

1 INTRODUCTION

In the current structure formation paradigm the properties of galaxies are coupled to the evolution of their dark matter (DM) hosting halo. For instance, the sizes and dynamics of galaxies are determined by the DM distribution inside a halo. This motivates the detailed study a DM halo internal structure.

The internal DM distribution in a halo can be parameterized through the density profile. In a first approximation this profile is spherically symmetric and its density only dependens on the radial coordinate. One the most popular radial parameterizations is the Navarro-Frenk-White (NFW) profile (Navarro et al. 1997). If one is not interested in the very central region of the dark matter halo (where galaxy formation takes place, and where the effects of baryon physics on dark matter distribution are still unknown) one can also assume that this profile is universal. (Navarro et al. 2010). This profile is a double power law in radius, where the transition break happens at the so-called scale radius, r_s. The ratio between the scale radius and the halo virial radius R_v is known as the concentration $c = R_v/r_s$.

The concentration of the NFW profile provides the conceptual framework to study simulated dark matter halos as a function of redshift and cosmological parameters. In many numerical studies (Neto et al. 2007; Macciò et al. 2008; Duffy et al. 2008; Muñoz-Cuartas et al. 2011; Prada et al. 2012; Ludlow et al. 2014) the results are summarized through the mass-concentration relationship; that is the distribution of concentration values at a fixed halo mass and redshift. The success of such numerical experiments rests on a reliable algorithm to estimate the concentration. Such an algorithm should provide unbiased results and must be robust when applied to simulations of different numerical resolution.

⋆ cn.poveda542@uniandes.edu.co
† je.forero@uniandes.edu.co
‡ juan.munozc@udea.edu.co

There are two main algorithms to estimate the concentration parameter of a N-body dark matter halo. The first method takes the halo particles and bins them into logarithmic radii to estimate the density in each bin, then it proceeds to fit the density as a function of the radius to the NFW profile. A second method uses an analytic property of the NFW profile that relates the maximum of the ratio of the circular velocity to the virial velocity, $V_{\rm circ}/V_{\rm vir}$. The concentration can be then found as the root of an algebraic equation dependent on this maximum value.

The first method is straightforward to apply but presents two disadvantages. First, it requires a large number of particles in order to have a proper density estimate in each bin. This makes the method robust only for halos with at least 10^3 particles. The second problem is that there is not a way to estimate the optimal radial bin size, different choices may produce different results for the concentration.

The second method solves the two problems mentioned above. It works with low particle numbers and does not involve data binning. However, it effectively takes into account only a single data point and discards the behaviour of the ratio $V_{\rm circ}/V_{\rm vir}$ below and above its maxima. Small fluctuations on the value of this maximum can yield large perturbations on the estimated concentration parameter.

In this letter we present a third alternative based on fitting the integrated mass profile. This approach has two advantages with respect to the above mentioned methods. It does not involve any data binning and does not throw away data points. This translates into a robust estimate even at low resolution/particle numbers. Furthermore, since the method does not require any binning, there is no need to tune numerical parameters. This provides a new independent method to estimate the concentration parameter. Here we provide a detailed description of the method and a comparison against the two traditional techniques by measuring its performance both on mock and N-body halos.

2 BASIC PROPERTIES OF THE NFW DENSITY PROFILE

Let us review first the basic properties of the NFW density profile. This shall help us to define our notation.

2.1 Density profile

The NFW density profile can be written as

$$\rho(r) = \frac{\rho_c \delta_c}{r/r_s(1+r/r_s)^2}, \tag{1}$$

where $\rho_c \equiv 3H^2/8\pi G$ is the Universe critical density, H is the Hubble constant, G and the universal gravitational constant, δ_c is the halo dimensionless characteristic density and r_s is the scale radius. This radius marks the point where the logarithmic slope of the density profile is equal to -2, the transition between the power law scaling $\rho \propto r^{-1}$ for $r < r_s$ and $\rho \propto r^{-3}$ for $r > r_s$.

We define the virial radius of a halo, r_v, as the boundary of the spherical volume that encloses a density of Δ_h times the mean density of the Universe. The corresponding mass M_v, the virial mass, can be written as $M_v = \frac{4\pi}{3}\bar{\rho}\Delta_h r_v^3$. From these virial quantities we define new dimensionless variables for the radius and mass $x \equiv r/r_v$ and $m \equiv M(<r)/M_v$.

In this letter we use $\Delta_h = 740$, a number roughly corresponding to 200 times the critical density at redshift z=0.

2.2 Integrated mass profile

From these definitions we can compute the total mass enclosed inside a radius r:

$$M(<r) = 4\pi\rho_c\delta_c r_s^3 \left[\ln\left(\frac{r_s+r}{r_s}\right) - \frac{r}{r_s+r}\right], \tag{2}$$

or in terms of the dimensionless mass and radius variables

$$m(<x) = \frac{1}{A}\left[\ln(1+xc) - \left(\frac{xc}{xc+1}\right)\right], \tag{3}$$

where

$$A = \ln(1+c) - \left(\frac{c}{c+1}\right), \tag{4}$$

and the parameter c corresponds to the concentration $c \equiv r_v/r_s$.

From this normalization and for later convenience we define the following function

$$f(x) = \ln(1+x) - \left(\frac{x}{x+1}\right). \tag{5}$$

The most interesting feature of Eq. (3) is that the concentration is the only free parameter to describe the integrated mass profile.

2.3 Circular velocity profile

It is also customary to express the mass of the halo in terms of the circular velocity $V_c = \sqrt{GM(<r)/r}$. From this we can define a new dimensionless circular velocity $v(<x) \equiv V_c(<r)/V_c(<r_v)$, using the result in Eq. 3 we have:

$$v(<x) = \sqrt{\frac{1}{A}\left[\frac{\ln(1+xc)}{x} - \frac{c}{xc+1}\right]}, \tag{6}$$

This normalized profile always shows a maximum provided that the concentration is larger than $c > 2$. It is possible to show that for the NFW profile the maximum is provided by

$$\max(v(<x)) = \sqrt{\frac{c}{x_{\rm max}}\frac{f(x_{\rm max})}{f(c)}}, \tag{7}$$

where $x_{\rm max} = 2.163$ (Klypin et al. 2014) and the function $f(x)$ correspondes to the definition in Eq. (5).

3 METHODS TO ESTIMATE THE CONCENTRATION FROM N-BODY SIMULATIONS

3.1 Estimates from the density and velocity profiles

To date, there are two standard methods to estimate concentrations in dark matter halos extracted from N-body simulations.

The first method tries to directly estimate the density profile. It takes all the particles in the halo and bins them in the logarithm of the radial coordinate from the halo center. Then, it estimates the density in each logarithmic bin counting the particles and dividing by the corresponding shell volume. At this point is possible to make a direct fit to the density as a function of the radial coordinate. This method has been broadly used for more than two decades to study the mass-concentration-redshift relation of dark matter halos.

A second method uses the circular velocity profile. It finds the value of x for which the normalized circular velocity $v(< x)$ shows a maximum. Using this value it solves numerically for the corresponding value of the concentration using Eq. (7). This method has been most recently used by Klypin et al. (2014) to study the mass-concentration-redshift relation using the Multidark Simulation Suite.

3.2 Our proposal: estimate from the integrated mass profile

Our method uses the integrated mass profile defined in Eq. (3). We build it from N-body data following the next steps. First, we define the center of the halo to be at the position of the particle with the lowest gravitational potential. Then we rank the particles by their increasing radial distance from the center. From this ranked list of $i = 1, N$ particles, the total mass at a radius r_i is $M_i = i \times m_p$, where r_i is the position of the i-th particle and m_p is the mass of a single computational particle. In this process we discard the particle at the center.

We divide the enclosed mass mass M_i and the radii r_i by their virial values to obtain the dimensionless variables m_i and x_i. Once the mass profile is expressed in dimensionless variables the concentration is the only free parameter. We then use an Affine Invariant Markov Chain Monte Carlo implemented in the python module *emcee* (Foreman-Mackey et al. 2013) to sample the likelihood function distribution defined by $\mathcal{L}(c) \propto \exp(-\chi^2(c)/2)$ where the $\chi^2(c)$ is written as

$$\chi^2(c) = \sum_{i=1}^{N} [\log m_i - \log m(< x_i; c)]^2, \tag{8}$$

where $m(< x_i; c)$ corresponds to the values in Eq.(3) at $x = x_i$ for a given value of the concentration parameter c and the i index sums over all the particles in the numerical profile. From the χ^2 distribution we find the optimal value of the concentration and its associated uncertainty.

4 RESULTS

We apply the three methods mentioned above on two different halo samples. The first sample is composed by mock halos generated to have known concentration values in perfect spherical symmetry following an NFW profile. Using this sample we want to quantify the ability to recover the expected concentration as a function of particle number. The second sample comes from a publicly available N-body cosmological simulation. In this way we test the new method on more realistic and complex data. We summarize the results on this dataset by showing the impact on the mass-concentration relationship.

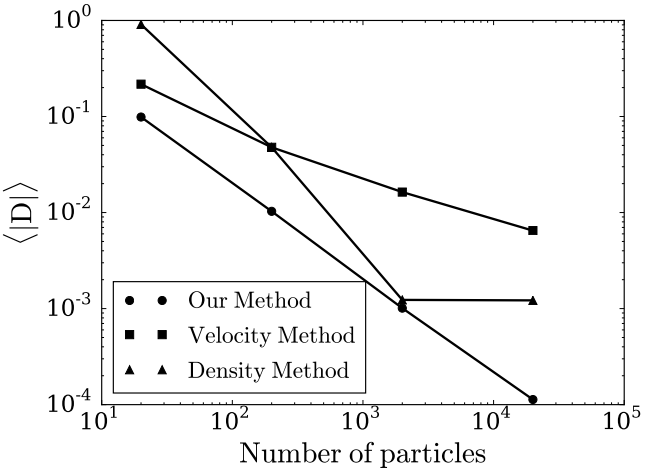

Figure 1. Average value of the relative error in the concentration estimate, $\langle |D| \rangle$, as a function of the particle number N in the set of mock halos. Different symbols represent different methods. Our method provide the most accurate estimate at fixed particle number N.

4.1 Mock halo sample

The method we use to generate the mock halos is based on the integrated mass profile. We start by fixing the desired concentration c and total number of particles N in the mock halo. With these values we define the mass element as $\delta m = 1/M$, corresponding to the mass of each particle such that the total mass is one. Then for each particle, $i = 1, \ldots, N$, we find the value of r_i such that the difference

$$m(< r_i; c) - i \cdot \delta m \tag{9}$$

is zero using Ridders' method.

The value of r_i is the radius of the i-th particle of the mock halo. Then we generate random polar and azimuthal angles θ and ϕ for each particle to ensure spherical symmetry. Finally these three spherical coordinates are transformed into Cartesian coordinates $(r, \theta, \phi) \rightarrow (x, y, z)$.

We generate in total 400 mock halos split into four different groups of 100 halos each. The four groups differ in the total number of particles for their halos: 20, 200, 2000 and 20000. Inside each group the halos have random concentration values in the range $1 < c < 20$ with a uniform distribution. We find the concentration values for all these halos using the density, velocity and integrated mass methods described in the previous section.

We quantify the difference between the expected c_{in} and measured c_{out} values by

$$D = (c_{in} - c_{out})/c_{in}, \tag{10}$$

and

$$\langle |D| \rangle = \frac{1}{|\mathcal{H}|} \sum_{\mathcal{H}} |D|, \tag{11}$$

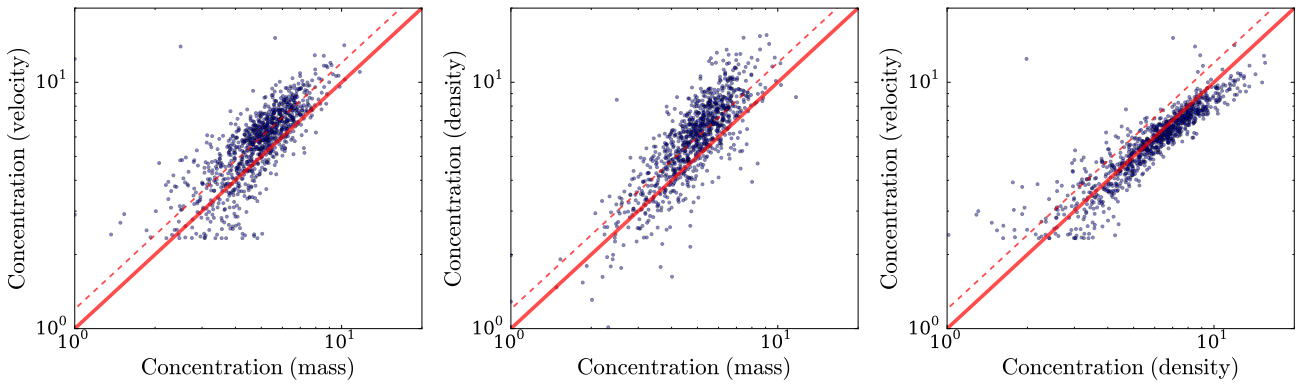

Figure 2. Comparison between the concentrations measured by our method and the maximum velocity (left) and density (middle) methods. The solid line indicates the equal value between the two techniques. The dashed line shows the upper 15 per cent difference between two methods.

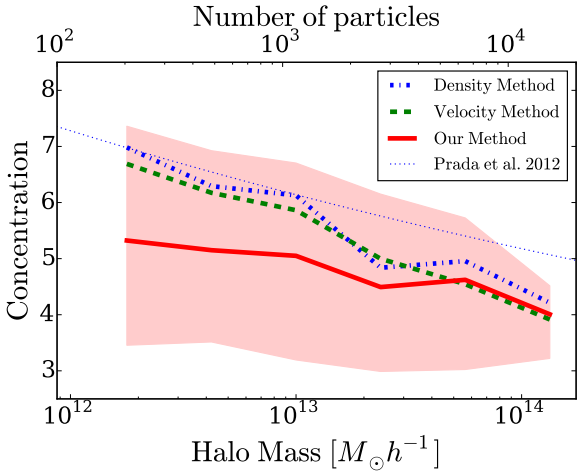

Figure 3. Mass-concentration relationship for the three different methods used on the same cosmological N-body data. All halos are used regardless of their relaxation state. The lines correspond to the median concentration values in each mass bin. The shaded region presents 10 and 90 per cent spread. For clarity we only show the spread for the concentrations estimated using our method. The other two methods have a similar spread. The dotted line corresponds to fits reported by (Prada et al. 2012).

where $\mathcal{H}$ corresponds to a set of mock halos, and $|\mathcal{H}|$ is the number of haloes in $\mathcal{H}$. A large discrepacy between the estimated and input concentrations are quantified by a large $\langle|D|\rangle$.

Figure 1 shows the behaviour of $\langle|D|\rangle$ as a function of halo particle number for the three different methods.

At fixed particle numbers our method always shows the lowest $\langle|D|\rangle$ values compared to the other two. Its accuracy is on the order of 10% for 20 particles in the halo, decreasing to 0.01% for halos with 20000 particles. The dependence of $\langle|D|\rangle$ with the particle number N goes approximately as $\langle|D|\rangle \propto N^{-1/2}$. This hints that the increasing accuracy of the method could be due to a decrease of Poisson noise.

The method based on the maximum of the circular velocity shows a similar behaviour with $\langle|D|\rangle \propto N^{-1/3}$. Its accuracy is $2-5$ times lower than in our method, on the order of 20% for 20 particle halos and 0.5% for 20000 particle halos. The method based on the direct density fit shows the lowest accuracy for a low particle number. As it is discussed in (Muñoz-Cuartas et al. 2011), density binning for halos with particle numbers below ~ 200 leads to a biased estimation of the mass density profile, and therefore to a biased estimation of the concentration parameter. This behaviour is evident in the large values of $\langle|D|\rangle$ for halos with number of particles below ~ 200 and an intermediate accuracy between the other two methods for a high particle number.

4.2 Halos from a cosmological simulation

The results presented in the previous section show that in an idealized setup (pure NFW desity profiles, perfect spherical halos in total isolation) our method performs better than the other two methods commonly used in the literature.

However, simulated dark matter halos in a cosmological context are complex. They are not isolated, many of them experience mergers that take them out of the equilibrium. Halos may have also plenty of substructure. All these effects disturb the mass density profile, taking it away from the ideal NFW profile. In order to explore the performance of our method in this setting, we use it to estimate the concentration parameter in dark matter halos obtained from a cosmological N-body simulation and compare with the other two classical methods.

We use data from the MultiDark cosmological simulation that follows the non-linear evolution of a dark matter density field sampled with 2048^3 particles over a cubic box of 1000 h^{-1}Mpc on a side. The data is publicly available at `http://www.cosmosim.org/`. More details about the structure of the database and the simulation can be found in (Riebe et al. 2013).

We use a halo sample containing all the halos located in a cubic sub-volume of 100 h^{-1}Mpc on a side centered on the most massive halo in the simulation at $z = 0$. This dataset corresponds to the `miniMDR1` table in the database. From this sample we select all the halos at $z = 0$ detected with a Friends-of-Friends (FoF) algorithm with masses in the interval $10^{12} \leqslant M_{\rm FoF}/h^{-1}{\rm M}_\odot \leqslant 10^{14}$. The FoF algorithm

used a linking length of 0.17 times the mean inter-particle distance. This choice translates into an overdensity $\Delta_h \sim 400 - 700$ dependent on the halo concentration (More et al. 2011). Finally, we select from the database all the particles that belong to each FoF group.

From this set of particles we follow the procedure spelled out in Section 3 with $\Delta_h = 740$ (corresponding to 200 times the critical density) to select an spherical region that we redefine to be our halo. This choice makes that our overdensities are fully included inside the original FoF particle group. On the interest of providing a fair comparison against the density method we only report results from overdensities with at least 200 particles.

Figure 2 shows the comparison between the concentration values obtained by the three different methods. The diagonal line marks a one-to-one correspondence if all the values were equal. The three methods show a broad general agreement. The largest difference is present at high concentration $c > 5$ where our method produces systematic lower values than the other two methods. Most of the differences are at the 20% level, with some extreme cases for the highest concentration values with 50% differences. The velocity and density methods produce consistent values within a 20% scatter, only some halos with very high concentrations $c \sim 10$ have a 15% lower concentration with the velocity method.

We explored halo shape and relaxation as a source of this differences. We found shape does not bias the concentration estimation; relaxation, quantified by the offset between the center of mass and minimum of the potential, can only explain at most 5% of the offset between methods. We note that the highest concentration values correspond to the smallest halos with ~ 200 particles, a regime where both the density and velocity methods are reliable only the 5% in a perfect spherical halo. This difference might actually signal a deviation from the NFW profile due to the low resolution in the simulation. From this we suggest that asserting with confidence the systematic difference between the different methods should be confirmed a higher resolution simulation and larger statistics. We leave this comparison for future work.

Figure 3 summarizes the previous results in the mass-concentration relationship.

We find that the median concentraion can be fit by the following relationship

$$c_{200} = 5.62 \left(\frac{M_{200}}{10^{12} h^{-1} \mathrm{M}_\odot} \right)^{-0.061}, \qquad (12)$$

which has a similar power value compared to the -0.075 reported by (Prada et al. 2012), while the normalization is $\sim 20\%$ lower compared to the 7.28 value reported by the same authors.

5 CONCLUSIONS

In this letter we presented a new method to estimate the concentration of dark matter halos in N-body simulations. We tested our method on mock halo data to study the impact of total number of particles and input concentration on the retrieved values. We compared these results against two other methods commonly used in the literature to estimate concentrations. Finally, we applied our method to halos extracted from a cosmological N-body simulation to estimate the impact of our method on the mass concentration relationship.

The first benchmark was performed on mock halos generated with known concentration values for different particle numbers. For all methods, the accuracy in retrieveing the input concentration increases with the number of particles as summarized in Figure 1. Our method systematically shows smaller errors in the retrieved values compared to the other two methods.

We used a N-body cosmological simulation to test the impact of our method on the mass-concentration relationship. Although the three methods are in general agreement there are some noticeable differences in the mass concentration relationship.

REFERENCES

Duffy A. R., Schaye J., Kay S. T., Dalla Vecchia C., 2008, MNRAS, 390, L64
Foreman-Mackey D., Hogg D. W., Lang D., Goodman J., 2013, PASP, 125, 306
Klypin A., Yepes G., Gottlober S., Prada F., Hess S., 2014, ArXiv e-prints
Ludlow A. D., Navarro J. F., Angulo R. E., Boylan-Kolchin M., Springel V., Frenk C., White S. D. M., 2014, MNRAS, 441, 378
Macciò A. V., Dutton A. A., van den Bosch F. C., 2008, MNRAS, 391, 1940
More S., Kravtsov A. V., Dalal N., Gottlöber S., 2011, ApJS, 195, 4
Muñoz-Cuartas J. C., Macciò A. V., Gottlöber S., Dutton A. A., 2011, MNRAS, 411, 584
Navarro J. F., Frenk C. S., White S. D. M., 1997, ApJ, 490, 493
Navarro J. F., Ludlow A., Springel V., Wang J., Vogelsberger M., White S. D. M., Jenkins A., Frenk C. S., Helmi A., 2010, MNRAS, 402, 21
Neto A. F., Gao L., Bett P., Cole S., Navarro J. F., Frenk C. S., White S. D. M., Springel V., Jenkins A., 2007, MNRAS, 381, 1450
Prada F., Klypin A. A., Cuesta A. J., Betancort-Rijo J. E., Primack J., 2012, MNRAS, 423, 3018
Riebe K., Partl A. M., Enke H., Forero-Romero J., Gottlöber S., Klypin A., Lemson G., Prada F., Primack J. R., Steinmetz M., Turchaninov V., 2013, Astronomische Nachrichten, 334, 691